Ultra-broadband polarization splitter based on graphene layer-filled dual-core photonic crystal fiber*

Hui Zou(邹辉)†, Hui Xiong(熊慧), Yun-Shan Zhang(张云山), Yong Ma(马勇), and Jia-Jin Zheng(郑加金)

College of Optoelectronic Engineering, Nanjing University of Posts and Telecommunications, Nanjing 210023, *China*

(Received 20 June 2017; revised manuscript received 24 July 2017; published online 20 November 2017)

An ultra-broadband polarization splitter based on graphene layer-filled dual-core photonic crystal fiber (GDC-PCF) that can work in a wavelength range from 1120 nm to 1730 nm is proposed in this paper. Through optimizing fiber configuration, the polarization splitter has an extinction ratio of −56.3 dB at 1.55 μm with a fiber length of 4.8 mm. Compared with the photonic crystal fiber reported splitters, to our knowledge, the GDC-PCF splitter with the extinction ratio below −20 dB has a super wide bandwidth of 610 nm. Due to the excellent splitting characteristics, the GDC-PCF will be used in coherent optical communication systems in a wavelength range from infrared to mid-infraed.

Keywords: polarization splitters, graphene, dual-core photonic crystal fiber

PACS: 42.81.–i, 42.79.Fm, 42.68.Mj, 63.22.Rc **DOI:** 10.1088/1674-1056/26/12/124216

1. Introduction

For photonic crystal fibers (PCFs), by changing the core and the hole configuration in cladding, compared with in the conventional fibers, the light propagation in PCFs are controlled extra freely, and many functional devices based on PCFs have attracted increasing attention, such as multiplexers,[1–3] couplers,[4,5] optics filters,[2,6] and splitters.[7–9] Among these devices, broadband polarization splitters based PCFs, which are capable of splitting the polarization of the incident light beam into two orthogonal states have also been used widely in optical communication systems in recent years.

In order to realize ultra-broadband polarization splitters with high extinction ratio (ER), until now, the main three kinds of methods have been reported in the literature as follows. Firstly, polarization properties of the PCFs are enhanced by changing core configuration. Early in 1990, Peng *et al.* demonstrated a polarization splitter based on a dual-elliptical-core optical fiber, and this splitter had a long length of 262 mm and operated at 633 nm.[10] But, this splitter was based on conventional fibers, resulting in small bandwidths. In 2003, Zhang and Yang[8] firstly proposed a polarization splitter based on a dual-core PCF. The structure of this dual-core PCF consists of three different sizes of air holes. Each core exhibited high birefringence, which gave rise to an adequate difference in coupling length between the two orthogonal polarizations. The polarization splitter possessed a splitting ratio better than −11 dB and a bandwidth of 40 nm.[8] In 2004, Saitoh *et al.* proposed a novel design of polarization splitter in three-core PCFs. The three-core PCF consisted of two given identical cores with two-fold symmetry separated by a core with high birefringence. The polarization splitter was based on the phenomenon of resonant tunneling. A 1.9-mm-long splitter with an extinction ratio better than −20 dB and a bandwidth of 37 nm was achieved. In 2011, Li *et al.* proposed a polarization splitter based on a dual-core hybrid PCF.[11] This kind of hybrid PCF had a large asymmetry resulting from the different light-guiding mechanisms in the orthogonal directions, the two polarized hybrid-guiding fundamental modes were no longer degenerate, and then high birefringence was achieved. The results demonstrated that a 4.72-mm-long polarization splitter with a bandwidth as wide as 190 nm and an ER better than −20 dB was obtained.[11]

Secondly, by changing cladding air hole configuration, polarization properties of the PCFs can be greatly improved. In 2006, a polarization splitter based on a three-core square-lattice PCF was proposed by Rosa and co-authors. By inserting different sizes of cladding air holes into the square lattice confirmation, the two-fold symmetry was formed, resulting in the input field changing into two orthogonally polarized beams with respect to the polarization axes. The splitter with 90 nm bandwidth and ER as low as −23 dB was achieved.[12] In 2013, Lu *et al.* have proposed a 400-nm or 300-nm bandwidth polarization splitter. Because of the introduction of two fluorine-doped cores and one elliptical or central microstructured modulation core modulation into seven cladding air hole rings, the symmetry of the PCF became twofold, and the asymmetries of the *x* and *y* directions were enhanced, the coupling length difference between the *x* polarization and *y* po-

*Project supported by the National Natural Science Foundation of China (Grant Nos. 61405096 and 61504058), the Introduction of Talent Research and Research Fund of Nanjing University of Posts and Telecommunications, China (Grant No. NY214158), the Open Fund of Laboratory of Solid State Microstructures, Nanjing University, China (Grant No. M28035), and the Open Fund of State Key Laboratory of Transient Optics and Photonics, Chinese Academy of Sciences (Grant No. SKLST201404).

†Corresponding author. E-mail: zouhui1010@163.com

© 2017 Chinese Physical Society and IOP Publishing Ltd

larization light was also increased. This meant that different-wavelength light could be separated totally at nearly the same distance. A polarization splitter was designed by choosing a certain fiber length at which the two polarization modes could be separated from each other and propagated in two cores, respectively, resulting in achieving an ultrawide band polarization splitter.[13,14] In 2015, Jiang *et al.*[15] proposed a polarization splitter with a bandwidth of 249 nm, whose structure consisted of seven rings of air holes, three elliptical air holes around the core, two different lattice constants and air hole diameters. The structure enhanced the birefringence, and resulted in a high coupling length difference between the x polarization and y polarization. It was feasible to design a high-performance polarization splitter.

Besides, polarization properties of the PCFs can be tailored by filling material or selecting coating metal. For example, in 2013, Sun *et al.* proposed a polarization splitter with a metal wire filled into a cladding air hole between the two cores, leading to extinction ratios as low as -20 dB with bandwidths as large as 146 nm.[16] In 2015, Jiang *et al.*[15] proposed a polarization splitter based on gold wire dual core PCFs, and integrated the gold wire between two cores; as a result, the 430-nm bandwidth of the splitter was effectively achieved.[15] In order to obtain ultra-broadband splitter, Abdul Khaleque *et al.*[17] proposed a novel configuration: a two elliptical and four larger air holes were introduced to enhance the birefringence, besides, gold filled dual core was embedded between the two elliptical air holes, as a result, the coupling length difference relating to x and y polarizations states was strengthen. This meant that the coupling length was relatively long and the polarization splitter was sensitive to wavelength. A 560-nm bandwidth polarization splitter was achieved.[17] In 2016, a polarization splitter based on the liquid crystal-filled dual-core photonic bandgap (PBG) holey fiber was investigated by Wang *et al.*[18] Through filling the liquid crystal into the air holes of a dual-core holey fiber with a simple structure and by setting appropriate geometrical parameters, the results demonstrated that the polarization splitter possessed a short length of 890.5 μm, and its wide bandwidth of $\sim$ 150 nm almost covered all the S, C, and L communication bands.[18]

According to the results from the above reported papers, in order to produce ultra-broadband splitter, it is better to have relatively flat coupling lengths of the two polarization states, and the value (the x and y polarization states coupling length ratio) is close to 2 or 1/2. In some of the designs and complex structures, the value is available by introducing the high birefringence characteristics or metal materials into the cladding of PCF. Especially, due to surface plasmons (SPs), which arise from the interaction between the evanescent electromagnetic fields and longitudinal collective oscillations of the free electrons in the metal, metal material is induced. The plasmonics on the PCF platform is excited. The properties of coupling and energy transfer are separately enhanced by the interaction between surface plasmon polariton (SPP) modes and guided core modes. Also, the plasmonic properties exist in the graphene layer.[18,19] More importantly, graphene exhibits the following characteristics: the high surface-to-volume ratio, ultra-broadband saturable absorption (from visible to infrared wavlength), plasmon waveguides and broadband polarizers.[20,21] In this article, an ultra-broadband polarization splitter is proposed, which is based on graphene layer-filled dual-core photonic crystal fiber (GD-PCF) with only four air hole rings. The compact polarization splitter operates in a very large bandwidth range from 1120 nm to 1730 nm. The proposed 4.8-mm-long polarization splitter with 610-nm broad-bandwidth could be used in optical communication and sensor systems.

2. Structure and theory

The cross-section of the GD-PCF polarization splitter is shown in Fig. 1. In order to create cores A and B, Two identical air holes located in the center on both sides are replaced with solid ones. The central air hole is filled with a graphene layer, and the thickness of graphene layer is t. The outer cladding includes four-layer air holes in a hexagonal array with lattice constant t. The diameter of air hole is d. The background material is pure silica,[21] of which the refractive index can be obtained from the Sellmeier formula. In our calculations, graphene is described by a complex refractive index $n(\lambda) = 3.0 + \mathrm{i}(C_1/3)\lambda$, where $C_1 = 5.446\ \mu\mathrm{m}^{-1}$.[22]

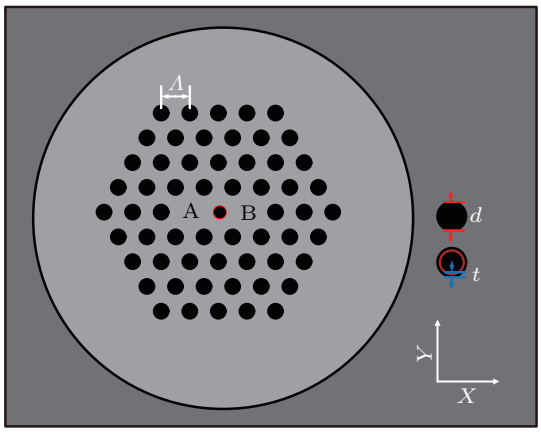


Fig. 1. (color online) The cross section of the proposed dual-core PCF. The gray area represents pure silica, the black circles denote air holes, the red annulus indicates graphene layer.

The coupled-mode theory is used to evaluate the performance and basic properties of the polarization splitter. According to the theory, the mode field of GD-PCF consists of four polarized modes, namely odd mode in the x polarization, even mode in the x polarization, odd mode in the y polarization and even mode in the y polarization. Modes with the same polarization produce mode coupling when they propagate along the fiber axis. The coupling length (CL) L_c, which is defined

as the distance (light power transfers from core A to core B completely), can be derived as

$$L_{\mathrm{c}}^{x,y} = \frac{\pi}{\beta_{\mathrm{even}}^{x,y} - \beta_{\mathrm{odd}}^{x,y}}. \tag{1}$$

Here, $\beta_{\mathrm{even}}^{x,y}$ and $\beta_{\mathrm{even}}^{x,y}$ are the propagation constants of the even modes and odd modes for the x polarization and the y polarization, respectively. The values of β can be calculated accurately by finite element method. The L_{c}^{x} and L_{c}^{y} usually are different due to the introduction of the birefringence. If the length of the fiber $= mL_{\mathrm{c}}^{x} = nL_{\mathrm{c}}^{y}$ (m and n are integers with opposite parities), the incident light with two orthogonal polarizations will totally exit at different ports (the x-polarization light mainly exists in one core, and the y polarization mainly exists in the other one). We define the ration $\delta = L_{\mathrm{c}}^{y}/L_{\mathrm{c}}^{x}$ as the coupling length ratio (CLR). Further, the ratio can be described as follows:

$$\delta = \frac{\beta_{\mathrm{even}}^{x} - \beta_{\mathrm{odd}}^{x}}{\beta_{\mathrm{even}}^{y} - \beta_{\mathrm{odd}}^{y}} = \frac{m}{n}. \tag{2}$$

In order to obtain a short length and excellent performance polarization splitter, optimal δ value is 2 or 1/2 (when $m = 2$, $n = 1$, $L_{\mathrm{c}}^{y} > L_{\mathrm{c}}^{x}$, $\delta = 2$; when $m = 1$, $n = 2$, $L_{\mathrm{c}}^{y} < L_{\mathrm{c}}^{x}$, $\delta = 1/2$). Assuming that the input port is core A, $P_{\mathrm{out},x}^{\mathrm{A}}$ and $P_{\mathrm{out},y}^{\mathrm{A}}$ are the output powers of x and y polarization in core A, are given by

$$P_{\mathrm{out},x}^{\mathrm{A}} = P_{\mathrm{in}} \cos^2\left(\frac{\pi L}{2L_{\mathrm{c}}^{x}}\right), \tag{3}$$

$$P_{\mathrm{out},y}^{\mathrm{A}} = P_{\mathrm{in}} \cos^2\left(\frac{\pi L}{2L_{\mathrm{c}}^{y}}\right). \tag{4}$$

Here, P_{in} is the power of the incident light, L_{c}^{x} and L_{c}^{y} can be acquired from Eq. (1). Besides, the extinction ratio (ER) in core A, which can defined as

$$\mathrm{ER} = 10\log_{10}\frac{P_{\mathrm{out},x}^{\mathrm{A}}}{P_{\mathrm{out},y}^{\mathrm{A}}}, \tag{5}$$

is considered to be the standard for measuring the performance of a polarization splitter. Commonly, as the ER is more than 20 dB, two perpendicular polarization states of light are deemed to be separated.

3. Numerical results and discussion

The full vectorial finite element method (FEM) providing high accuracy and flexible triangular meshes is implemented to characterize the proposed GD-PCF polarization splitter. In order to investigate its polarization properties, the dispersion relations of the first and second order SPP modes[19,20] and four super-modes are numerically calculated and shown in Fig. 2. According to Fig. 2(a), we can clearly see that for wavelengths shorter than 1 μm, the x- and y-polarized supermodes are nearly degenerate (e.g., x-, y-odd, and x-, y-even modes have nearly the same effective indices), although the refractive indices for even and odd modes are different. However, at 0.905 μm, the plasmonic mode is generated, for the surface plasmon resonance of the grapheme layer is produced at the interface between the graphene layer and the central air hole,[19,20] the 2nd order plasmon polarization (SPP) mode is also excited. But, compared with the core supermode, the first order SPP mode is omitted because of its high effective refractive index. As shown in the insert of Fig. 2(a), when the real part of the effective index of core guided modes matches with the plasmonic mode, the resonant coupling between the cores guided mode and the plasmonic mode is enhanced. The effective index of the y-odd mode matches with the 2nd SPP mode, and there is a coupling between two, leading to a split of the effective index of this mode with respect to its degenerate x-odd mode, this is not strongly affected by the 2nd SPP mode.

Meanwhile, the third (or higher) order SPP mode is omitted due to its low effective refractive indice compared with the core super mode, i.e., there is no coupling between the core super mode and the first order SPP mode, and the interaction between its mode and the core supermode is weak as shown in Fig. 2(b). Besides, for the first order SPP mode, its effective refractive index is higher but lower than that for the core supermode. And the interaction among them is non-existent. Then, the even modes (x- and y-polarized modes) are not strongly affected by the first order SPP mode.

For the dual-core PCF without graphene, the even and odd modes (x- and y-polarized modes) are not affected by the 2nd SPP mode, the x- and y-odd modes are not changed as the wavelength increases in Fig. 2(c). As the wavelength increases, the effective refractive index difference of x- and y-polarization modes increases linearly and uniformly in the insert of Fig. 2(c). Just contrarily, the graphene layer is filled into the center hole of the dual-core PCF, the coupling between the y-odd mode and the 2nd SPP mode is produced, and the x- and y-odd modes become more and more separated as the wavelength increases in Fig. 2(d). The effective refractive index difference of x- and y-polarization modes increases nonlinearly and uniformly with increasing wavelength in the insert of Fig. 2(d). The difference increases to a maximum value, then decreases, then increases with increasing wavelength, and the range of its variation is relatively large, especially the variation range of the polarization state in the y direction. The difference between L_{c}^{x} and L_{c}^{y} is also greatly changed. As shown in Fig. 2(d), it indicates that the difference in odd-mode refractive indice in y-polarized direction can be modulated by the coating of grapheme layer. The modulation intensity in the y-polarized direction is greater than in the x-polarized direction. The even modes (x- and y-polarized) modes are not strongly

affected by the 2nd SPP mode because they are significantly better confined in cores A and B and therefore do not strongly interact with the graphene coating layer. It is shown in Fig. 3 that the even-mode polarized light is less affected by the surface plasmon mode, but the odd-mode polarized light is more greatly influenced, especially in the y direction of odd mode.

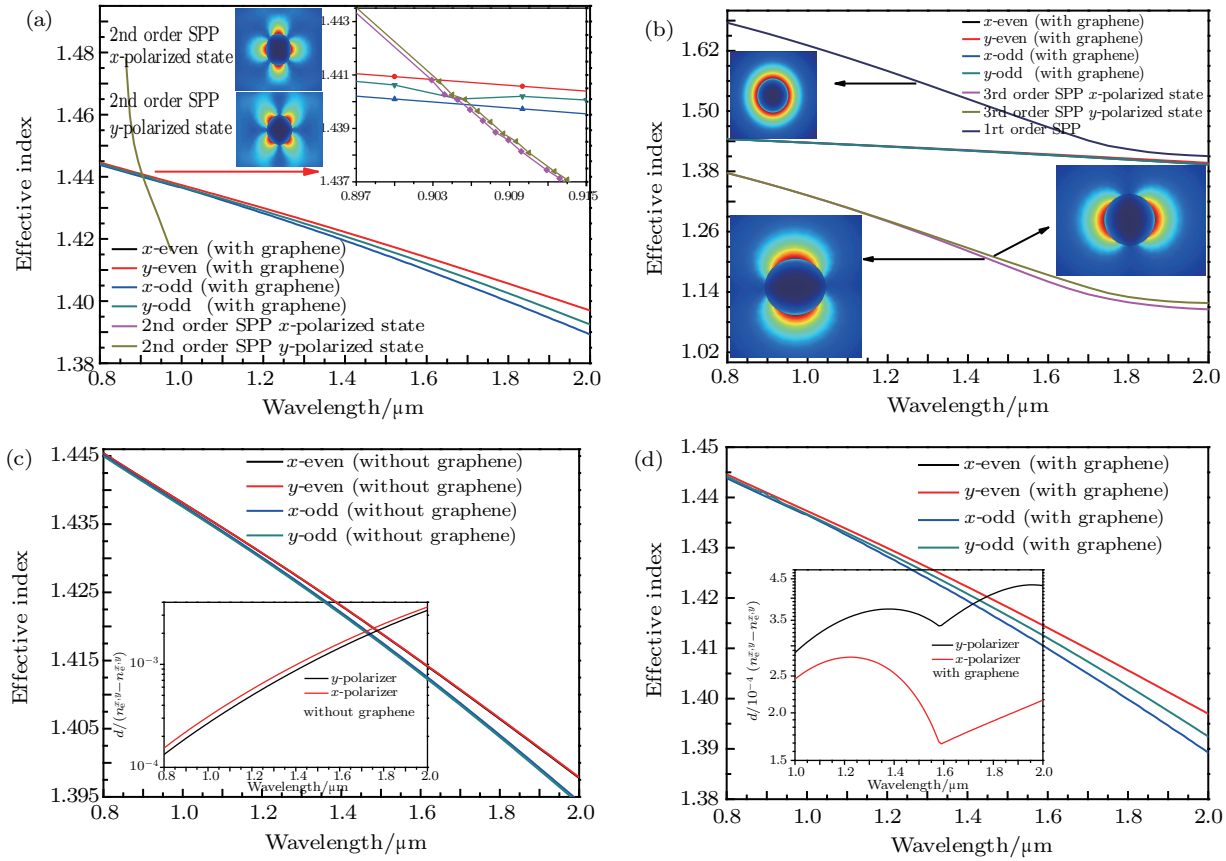


Fig. 2. (color online) Plots of effective refractive indices of (a) the supermodes and 2nd order SP modes and (b) 1rt–3rd order SP modes versus wavelength for the grapheme layer filled dual-core photonic crystal polarizer; plots of effective refractive index of the even/odd mode versus wavelength for the dual-core photonic crystal (c) without and (d) with the grapheme layer. The inset is a zoom-in view showing the effective refractive index difference of x- and y-polarization mode on a log scale versus wavelength.

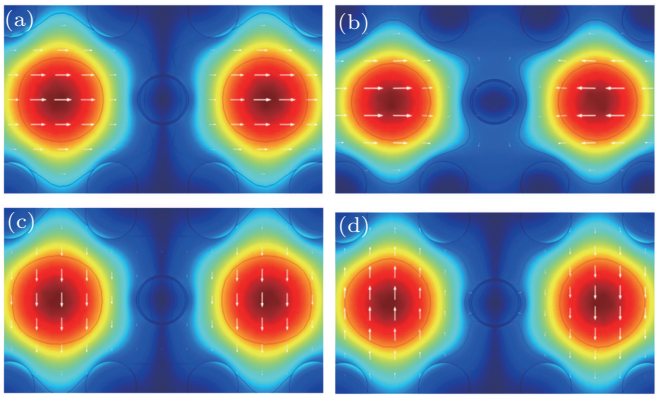


Fig. 3. (color online) Electrical field distributions of the dual-core PCF with the graphene layer at 1.55 μm: (a) even mode of x polarization; (b) odd mode of x polarization; (c) even mode of y polarization; (d) odd mode of y polarization.

The conventional dual-core PCF usually exhibits small difference in coupling length between the two orthogonal polarized directions, i.e., the coupling length ratio δ is nearly 1. In order to obtain an optimal δ ($\delta = 2$), a graphene coating is employed on the surface of the central air hole, and the technology of surface plasmon resonance is used, the 2nd SPP mode is produced and interacts with the even modes, resulting in enhancing the difference in coupling length. As shown in Fig. 4, compared with traditional dual-core PCF, the dual-core PCF with graphene layer possess the different characteristics. Figure 4(a) shows variations of CL and CLR for x and y polarizations with wavelength for the optimized structural parameters with a graphene layer. To verify the effect of the graphene layer on CL/CLR, the characteristics of the dual-core PCF without a graphene layer in the center are described in Fig. 4(b). In the absence of graphene layer, the value of CLR decreases with the increase of wavelength CLR that has a maximum value of 1.14, making it hard to split the two polarization modes to different cores. However, with the addition of the graphene layer, the value of CLR increases with the increase of wavelength, it is easy to achieve CLR = 2, meaning that when the beam is maximum in core A for the x-polarized mode, the y-polarized mode is nearly completely transferred to core B, resulting in an effective splitting of the modes. Hence, the graphene layer plays an important role in the excitations of plasmonic waves and the coupling difference between the x-

and y-polarized modes is enhanced. The GD-PCF possesses higher coupling length ratio.

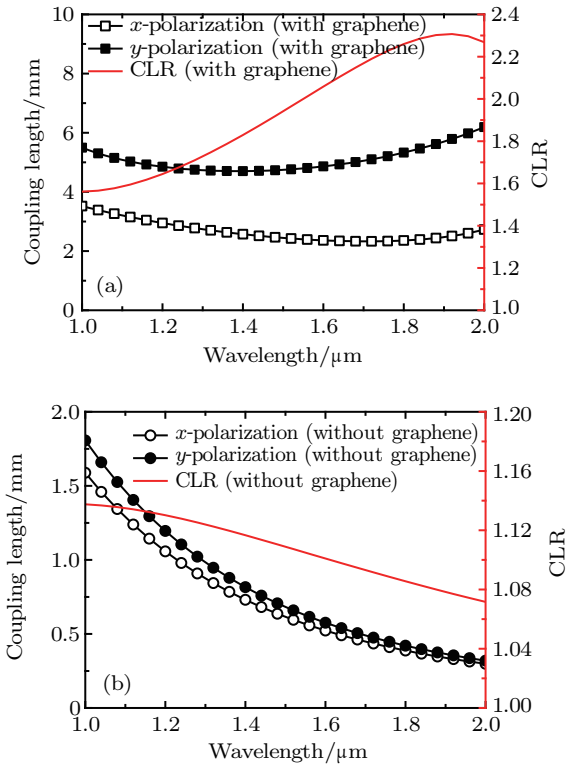


Fig. 4. (color online) Plots of coupling length and coupling length ratios versus wavelength for the proposed structure (a) with graphene and (b) without graphene.

The reason for the phenomenon can be explained as follows. The effective refractive index (n_{eff}) of the 2nd-SPP mode, i.e., mode at graphene layer interface, interferes with the core-guided fundamental modes in DC-PCF without graphene layer. Resonance occurs when the real part of the effective index of core guided mode matches with the plasmonic mode. The matched mode is obtained and leads to strongest coupling. It can be seen in Fig. 2 that the dispersion curves of the x-polarized and y-polarized supermodes are continuous at a given wavelength, except the region where the supermodes and 2nd order SPP modes match with each other. At $\lambda = 0.905$ μm, the effective indices of a 2nd order SPP mode and the y-polarized odd supermode match with each other. As a result, the difference in coupling length between x and y polarization modes is caused by resonance with SPP mode whose parity matches with each other. In addition, at $\lambda = 1.55$ μm, the coupling length ratio is very close to 2 in Fig. 4(a), this enables the possibility of achieving a high performance splitter by employing the GD-PCF.

In our work, the best option of the geometrical parameters of the proposed fiber is set to be $d = 1$ μm, $\Lambda = 2.2$ μm, $t = 45.6$ nm. Numerical results demonstrates coupling length ratio $\delta = 2.0004$ at a wavelength of 1.55 μm. Obviously, a high performance polarization splitter can be achieved by setting the fiber length to be $L = 4.8$ mm. Supposing that the input port is core A, the variations of the normalized transmission power with propagation distance for different polarizations can be obtained from Eqs. (3) and (4) as shown in Fig. 5 at the wavelength of 1.55 μm . Apparently, the output power for x polarization reaches a maximum while the power for y polarization is close to zero at a propagation distance of 4.8 mm, i.e., the two polarizations are separated at the length of 4.8 mm. Taking the confinement loss into consideration, the splitter exhibits a corresponding loss of 0.5 dB.

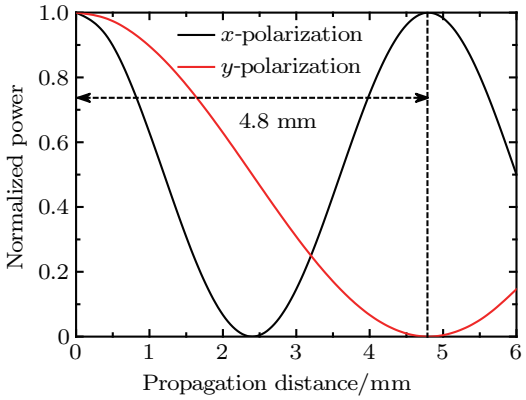


Fig. 5. (color online) Normalized powers for x and y polarization versus propagation distance at 1.55 μm.

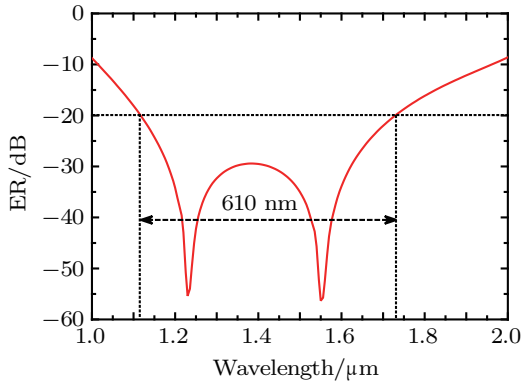


Fig. 6. (color online) Wavelength dependence of extinction ratio for the optimal parameters.

The extinction ratio (ER) is considered to be the standard for measuring the performance of a polarization splitter. Commonly, two perpendicular polarization states of light are deemed to be separated as the ER is more than 20 dB. Assuming that the incident light enters into core A, the ER of output port A is defined as

$$\text{ER} = 10\log_{10}\frac{P^{\text{A}}_{\text{out},x}}{P^{\text{A}}_{\text{out},y}}, \tag{6}$$

where $P^{\text{A}}_{\text{out},x}$ and $P^{\text{A}}_{\text{out},y}$ can be obtained from Eqs. (3) and (4), respectively. Figure 6 shows the extinction ratio as a function of wavelength, with the device length being 4.8 mm. The polarization splitter possesses high extinction ratio at the wavelengths of 1.55 μm and 1.23 μm, the corresponding values are −56.3 dB and −55.4 dB. In addition, the bandwidth of the splitter is 610 nm, i.e., from 1120 nm to 1730 nm, covering all

the O, E, S, C, L, and U bands. We also summarize the performances of the proposed polarization splitter and other polarization splitters, in terms of extinction ratio at 1550 nm, bandwidth, and working spectral region as indicated in Table 1. As can be seen, our splitter has advantage in bandwidth compared with reported splitters.

Table 1. Comparison of performance between the proposed fiber and other polarization splitters.

Reference	Extinction ratio at 1550 nm/dB	Bandwidth/nm	Working spectral region/nm
[12]	–23	90	1450–1540
[8]	–11	40	1525–1565
[14]	–25	400	1270–1670
[6]	–30	300	1340–1640
[24]	–118.7	249	1417–1666
[17]	–111	560	1420–1980
Our splitter	–56.3	610	1120–1730

4. Conclusions

In this paper, an ultra-broadband and simple-structure polarization splitter based on dual-core PCF with graphene layer is proposed. Simulation results indicate that the polarization splitter has an extinction ratio of −56.3 dB at 1.55 μm with a fiber length of 4.8 mm. More importantly, our splitter shows an ultra-broadband width of 610 nm (from 1120 nm to 1730 nm), with an extinction ratio below −20 dB. Due to the excellent splitting characteristics, the proposed GDC-PCF will be a promising candidate for coherent optical communication systems.

References

[1] Suzuki K, Kubota H, Kawanishi S, TanakaM and Fujita M 2001 *Electron. Lett.* **37** 1399
[2] Kakarantzas G, Ortigosa-Blanch A, Birks T, Russell P S J, Farr L Couny F and Mangan B 2003 *Opt. Lett.* **28** 158
[3] Tajima K, Zhou J, Nakajima, K and Sato K 2004 *J. Lightwave Technol.* **22** 7
[4] Lee B H, Eom J B, Kim J, Moon D S, Paek U C and Yang G H 2002 *Opt. Lett.* **27** 812
[5] Saitoh K, Sato Y and Koshiba M 2003 *Opt. Express* **11** 3188
[6] Ortigosa Blanch A, Knight J, Wadsworth W, Arriaga J, Mangan B, Birks T, Russell and P S J 2000 *Opt. Lett.* **25** 1325
[7] Zhang L and Yang C 2004 *IEEE Photon. Technol. Lett.* **16** 1670
[8] Zhang L and Yang C 2003 *Opt. Express* **11** 1015
[9] Saitoh K, Sato Y and Koshiba M 2004 *Opt. Express* **12** 3940
[10] Peng G, Tjugiarto and T Chu P 1990 *Electron. Lett.* **26** 682
[11] Li J, Wang J, Wang R and Liu Y 2011 *Opt. Laser Technol.* **43** 795
[12] Rosa L, Poli F, Foroni M, Cucinotta A and Selleri S 2006 *Opt. Lett.* **31** 441
[13] Lu W, Lou S, Wang X, Wang L and Feng R 2013 *Appl. Opt.* **52** 449
[14] Lu W, Lou S and Wang X 2013 *Appl. Opt.* **52** 8494
[15] Jiang L, Zheng Y, Hou L, Zheng K, Peng and J Zhao X 2015 *Opt. Commun.* **50** 56
[16] Sun B, Chen M Y, Zhou J and Zhang Y K 2013 *Plasmonics* **8** 1253
[17] Khaleque and Hattori H T 2015 *J. Appl. Phys.* **118** 143101
[18] Wang E L, Jiang H M, Xie K, Chen C and Hu Z J 2016 *J. Appl. Phys.* **120** 114501
[19] Dash J N and Jha R 2014 *IEEE Photon. Technol. Lett.* **26** 1092
[20] Maharana P K, Srivastava T and Jha R 2013 *IEEE Photon. Technol. Lett.* **25** 122
[21] Nair R, Blake P, Grigorenko A, Novoselov K, Booth T, Stauber T, Peres N and Geim A 2008 *Science* **320** 1308
[22] Guan C, Li S, Shen Y, Yuan T, Yang J and Yuan L 2015 *J. Lightwave Technol.* **33** 349
[23] Agrawal G P 2007 *Nonlinear Fiber Optics*, 4th edn. (Academic Press)
[24] Pospischil A, Humer M, Furchi M M, Bachmann D, Guider R and Fromherz T and Mueller T 2013 *Nat. Photon.* **7** 892
[25] Jiang H, Wang E, Zhang J, Hu L, Mao Q, Li Q and Xie K 2014 *Opt. Express* **22** 30461